Pseudo and quasi quark PDF in the BFKL approximation

Giovanni Antonio Chirilli

University of Santiago de Compostela

Color Glass Condensate at the electron-ion collider

ECT* Trento - Italy

15 - 19 May 2023

Primordial idea

$$\langle P|\bar{\psi}(x^+)\gamma^+[x^+,0]\psi(0)|P\rangle \quad \to \quad \langle P|\bar{\psi}(z)\gamma^3[z,0]\psi(0)|P\rangle + \mathcal{O}\left(\frac{\Lambda^2}{(P^3)^2}\right)$$

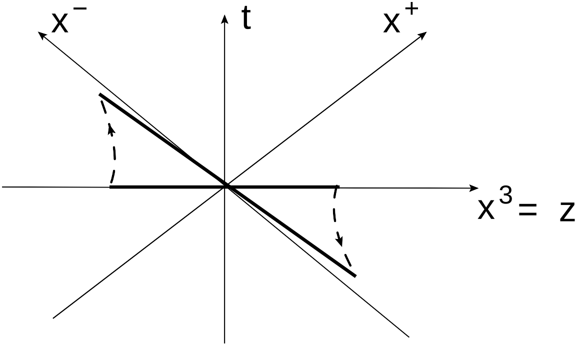

$x^{\pm} = \frac{x^0 \pm x^3}{\sqrt{2}}$

Lattice calculation

Ioffe-time $\varrho \equiv z \cdot P$ $\quad z^2 \neq 0$

$$M^\alpha(z,P) \equiv \langle P|\bar{\psi}(z)\gamma^\alpha[z,0]\psi(0)|P\rangle$$

$$M^\alpha(z,P) = 2P^\alpha \mathcal{M}(\varrho, z^2) + 2z^\alpha \mathcal{N}(\varrho, z^2)$$

- The pseudo-ITD $\mathcal{M}(\varrho, z^2)$ contains (not only) the leading twist term
- $\mathcal{N}(\varrho, z^2)$ contains higher twists terms
- higher twist: $\mathcal{O}(z^2\Lambda_{QCD})$
- $P = (E, 0, 0, P^3) \qquad z = (0, 0, 0, z^3)$;
  - for $\alpha = 0$ one isolate $\mathcal{M}(\varrho, z^2)$.

Lattice calculation

Ioffe-time $\varrho \equiv z \cdot P$ $\qquad z^2 \neq 0$

$$M^\alpha(z,P) \equiv \langle P|\bar{\psi}(z)\gamma^\alpha[z,0]\psi(0)|P\rangle$$

$$M^\alpha(z,P) = 2P^\alpha \mathcal{M}(\varrho,z^2) + 2z^\alpha \mathcal{N}(\varrho,z^2)$$

- Reduced pseudo-ITD removes the UV divergences.

$$\mathfrak{M}(\varrho,z^2) = \frac{\mathcal{M}(\varrho,z^2)}{\mathcal{M}(0,z^2)}$$

- Logarithmic singularity $\ln(-z^2)$ in $\mathfrak{M}(\varrho,z^2)$ (and in $\mathcal{M}(\varrho,z^2)$)
  - $\Rightarrow$ DIS logarithmic scaling violation with respect to the photon virtuality Q^2.

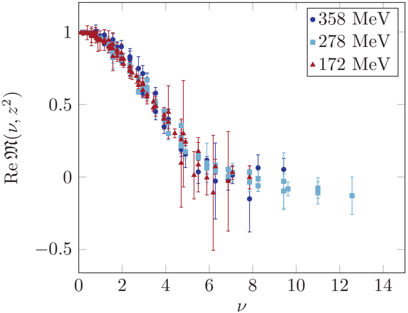

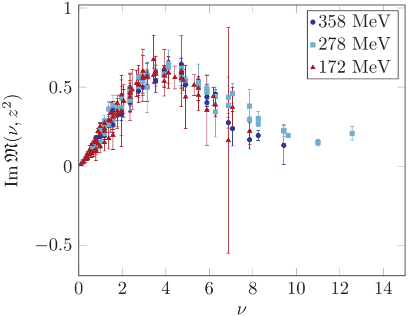

Phys.Rev.Lett. 125 (2020) 23, 232003

Ioffe-time $\nu \equiv z \cdot P$ z^μ space-like vector $i = 1, 2$

This talk: $\nu \to \varrho$

Definition of the pseudo and quasi quark PDF

Pseudo Ioffe-time distribution

$$\mathcal{M}(\varrho, z^2) \equiv \frac{z_\mu}{2\varrho}\langle P|\bar{\psi}(z)\gamma^\mu[z,0]\psi(0)|P\rangle$$

Ioffe-time $\varrho \equiv z \cdot P$ $\quad$ z^μ space-like vector $\quad$ $i = 1, 2$

Ioffe-time distribution at high energy

$$\langle P|\bar{\psi}(L, x_\perp)\gamma^-[Ln^\mu + x_\perp, 0]\psi(0)|P\rangle$$

Definition of the pseudo and quasi quark PDF

Ioffe-time $\varrho \equiv z \cdot P$ z^μ space-like vector $i = 1, 2$

Pseudo-PDF: Fourier transform with respect to P keeping its orientation fixed

$$Q_{\rm p}(x_B, z^2) = \int \frac{d\varrho}{2\pi}\, e^{-i\varrho x_B} \mathcal{M}(\varrho, z^2)$$

Quasi-PDF: Fourier transform with respect to z keeping its orientation fixed

$$Q_q(x_B, P_\xi) = P_\xi \int \frac{d\varsigma}{2\pi}\, e^{-i\varsigma P_\xi x_B} \mathcal{M}(\varsigma P_\xi, \varsigma^2)$$

$\xi^\mu = \frac{z^\mu}{|z|}$ $P_\xi = P \cdot \xi$

DIS at Leading Log Approximation at high-energy

$$T\{\hat{j}_\mu(x)\hat{j}_\nu(y)\} = \int d^2z_1 d^2z_2\; I^{\rm LO}_{\mu\nu}(z_1,z_2,x,y)\mathrm{Tr}\{\hat{U}^\eta_{z_1}\hat{U}^{\dagger\eta}_{z_2}\}$$

- Calculate LO Impact factor: $I^{\rm LO}_{\mu\nu}(z_1,z_2,x,y)$
- Calculate evolution of matrix element $\mathrm{Tr}\{\hat{U}^\eta_{z_1}\hat{U}^{\dagger\eta}_{z_2}\}$: BK/JIMWLK equation
  - we need only linear terms: BFKL
- Solve the evolution equation with initial condition: GBW/MV model
- Convolute the solution of the evolution equation with the impact factor

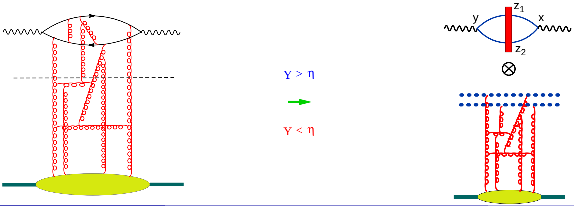

High-energy OPE for Ioffe-time distribution

$$\langle P|\bar{\psi}(x)\gamma^-[x,0]\psi(0)|P\rangle = \int d^2z_2 d^2z_z\, I_q(z_1,z_2;x)\langle P|\mathrm{tr}\{U(z_1)U^\dagger(z_2)\}|P\rangle$$

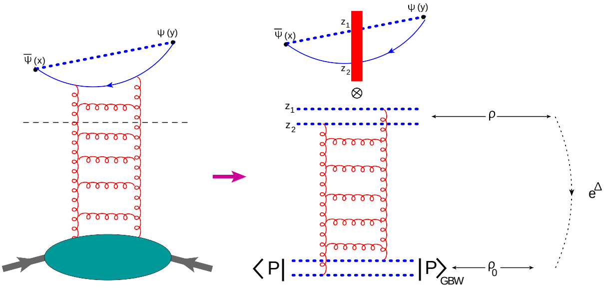

- Calculate coefficient functions (impact factors) I_q
- Convolute them with the solution of the evolution equation of relative matrix elements

High-energy operator product expansion

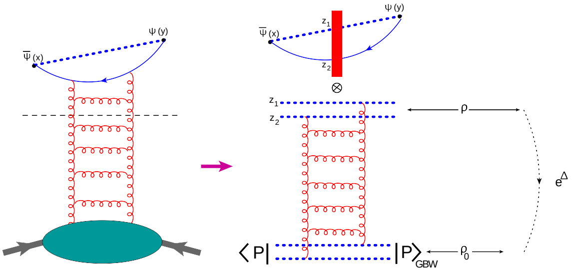

Resum $\alpha_s \ln \varrho$ with BFKL eq. $a = -\frac{2x^+y^+}{(x-y)^2 a_0}$

$$2a\frac{d}{da}\,\mathcal{V}_a(z_\perp) = \frac{\alpha_s N_c}{\pi^2}\int d^2z'\Big[\frac{\mathcal{V}_a(z'_\perp)}{(z-z')^2_\perp} - \frac{(z,z')_\perp \mathcal{V}_a(z_\perp)}{z'^2_\perp (z-z')^2_\perp}\Big]$$

solution $\mathcal{V}^a(z_{12}) = \int \frac{d\nu}{2\pi^2}(z_{12}^2)^{-\frac{1}{2}+i\nu}\left(\frac{a}{a_0}\right)^{\frac{\aleph(\gamma)}{2}} \int d^2\omega(\omega_\perp^2)^{-\frac{1}{2}-i\nu}\mathcal{V}^{a_0}(\omega_\perp)$

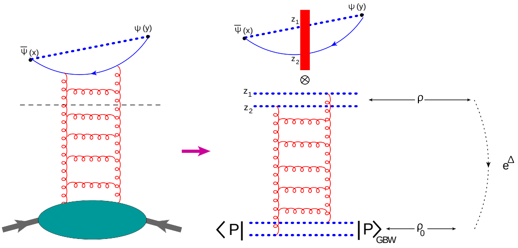

Saddle point approximation

$$\mathcal{M}(\varrho, z^2) \simeq \frac{i N_c}{64} \frac{Q_s \sigma_0}{|z|} \left(\frac{2\varrho^2}{z^2 M_N^2} + i\epsilon \right)^{\bar{\alpha}_s 2 \ln 2} \frac{e^{-\frac{\ln^2 \frac{Q_s |z|}{2}}{7\zeta(3)\bar{\alpha}_s \ln\left(\frac{2\varrho^2}{z^2 M_N^2} + i\epsilon\right)}}}{\sqrt{7\zeta(3)\bar{\alpha}_s \ln\left(\frac{2\varrho^2}{z^2 M_N^2} + i\epsilon\right)}}$$

saturation scale Q_s , $\sigma_0 = 29.1$ mb , M_N mass of the nucleon

Plot of the Ioffe-time amplitude in BFKL approximation

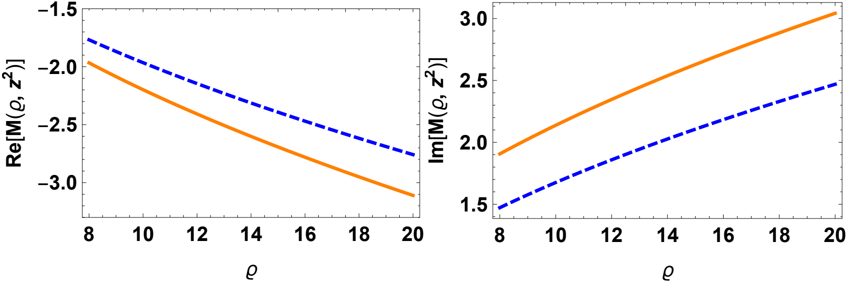

Figure : In the left and right panel we plot the real and imaginary part, respectively, of the Ioffe-time amplitude; we compare the numerical evaluation with its saddle point approximation (blue dashed curve). To obtain the plots we used $|z| = 0.5$, and $M_N = 1$ GeV.

Pseudo-PDF from Ioffe-time distribution

Pseudo-PDF: Fourier transform with respect to $z \cdot P$

$$Q_{\rm p}(x_B, z^2) = \int \frac{d\varrho}{2\pi}\, e^{-i\varrho\, x_B} \mathcal{M}(\varrho, z^2)$$

$$Q_{\rm p}(x_B, z^2) = -\frac{i\, N_c Q_s \sigma_0}{4\pi^2 |z| x_B} \int d\nu \left(\frac{2}{z^2 M_N^2 x_B^2} + i\epsilon \right)^{\frac{\aleph(\gamma)}{2}} \sin\left[\frac{\pi}{2}\aleph(\gamma)\right]$$
$$\times \frac{\gamma^2\, \Gamma(1+\aleph(\gamma))}{\sin^2(\pi\gamma)} \frac{\Gamma(1+\gamma)}{\Gamma(2+2\gamma)} \left(\frac{Q_s^2 x_\perp^2}{4}\right)^{i\nu}$$

Let's take saddle point approximation

Pseudo-PDF from Ioffe-time distribution

Pseudo-PDF: Fourier transform with respect to $z \cdot P$

$$\mathcal{Q}_{\rm p}(x_B, z^2) = \int \frac{d\varrho}{2\pi}\, e^{-i\varrho\, x_B} \mathcal{M}(\varrho, z^2)$$

Saddle point approximation

$$\mathcal{Q}_{\rm p}(x_B, z^2) \simeq -\frac{i N_c Q_s \sigma_0 \bar{\alpha}_s \ln 2}{32|z||x_B|} \frac{e^{\frac{-\ln^2 \frac{Q_s|z|}{2}}{7\zeta(3)\bar{\alpha}_s \ln\left(\frac{2}{x_B^2 z^2 M_N^2} + i\epsilon\right)}}}{\sqrt{7\zeta(3)\bar{\alpha}_s \ln\left(\frac{2}{x_B^2 z^2 M_N^2} + i\epsilon\right)}} \left(\frac{2}{x_B^2 z^2 M_N^2} + i\epsilon\right)^{\bar{\alpha}_s 2\ln 2}$$

Plot of the quark pseudo-PDF

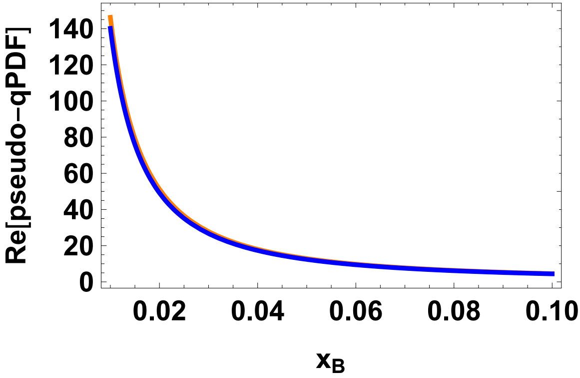

Figure : The plot presents the quark pseudo PDF by comparing the numerical evaluation (illustrated by the orange curve) with its saddle point approximation (portrayed by the blue curve).

Quasi-PDF from Ioffe-time distribution

Quasi-PDF: Fourier transform with respect to z^μ keeping its orientation fixed

$$Q_q(x_B, P_\xi) = P_\xi \int \frac{d\varsigma}{2\pi}\, e^{-i\varsigma\, P_\xi x_B} \mathcal{M}(\varsigma P_\xi, \varsigma^2)$$

$\xi^\mu = \frac{z^\mu}{|z|}$ $\qquad P_\xi = P \cdot \xi$

$$\begin{aligned} Q_{\rm q}(x_B, P_\xi) = & \int_{-\infty}^{+\infty} d\varsigma\, e^{-i\varsigma P_\xi x_B} \frac{i N_c P_\xi}{4\pi|\varsigma|} Q_s \sigma_0 \\ & \times \int d\nu \left(-\frac{2P_\xi^2}{M_N^2} + i\epsilon\right)^{\frac{\aleph(\gamma)}{2}} \frac{\Gamma^2(1-\gamma)\Gamma^3(1+\gamma)}{\pi^3\Gamma(2+2\gamma)} \left(\frac{Q_s^2|\varsigma|^2}{4}\right)^{i\nu} + \mathcal{O}(\alpha_s) \end{aligned}$$

and the saddle point approximation is

Quasi-PDF from Ioffe-time distribution

Quasi-PDF: Fourier transform with respect to z^μ keeping its orientation fixed

$$Q_q(x_B, P_\xi) = P_\xi \int \frac{d\varsigma}{2\pi}\, e^{-i\varsigma\, P_\xi x_B} \mathcal{M}(\varsigma P_\xi, \varsigma^2)$$

$\xi^\mu = \frac{z^\mu}{|z|} \qquad P_\xi = P \cdot \xi$

$$Q_{\rm q}(x_B, P_\xi) \simeq \frac{i N_c P_\xi Q_s \sigma_0}{64\pi} \left(-\frac{2P_\xi^2}{M_N^2} + i\epsilon\right)^{\bar{\alpha}_s 2 \ln 2}$$

$$\times \int_{-\infty}^{+\infty} \frac{d\varsigma}{|\varsigma|}\, e^{-i\varsigma P_\xi x_B} \frac{e^{-\frac{\ln^2 \frac{Q_s|\varsigma|}{2}}{7\zeta(3)\bar{\alpha}_s \ln\left(-\frac{2P_\xi^2}{M_N^2} + i\epsilon\right)}}}{\sqrt{7\zeta(3)\bar{\alpha}_s \ln\left(-\frac{2P_\xi^2}{M_N^2} + i\epsilon\right)}}$$

Plot of the quark quasi-PDF

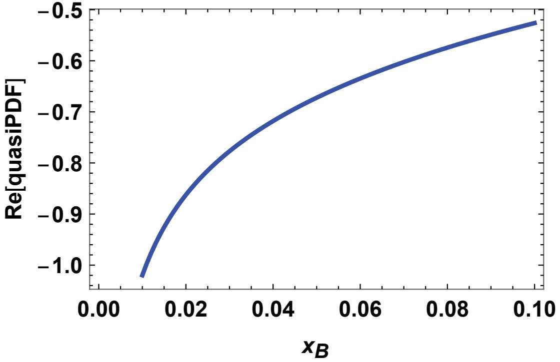

Figure : Plot of the real part of the numerical evaluation with $P_\xi = 4$ GeV, $\bar{\alpha}_s = 0.2$, and $M_N = 1$ GeV.

n-th moment of the structure function

The Q^2 behavior of DIS structure function is obtained from the anomalous dimension of twist-two operators

$$\mu\frac{d}{\mu}F^a_{\xi+}\nabla_+^{n-2}F^{a\,\xi}_{+} = \gamma(\alpha_s, n)F^a_{\xi+}\nabla_+^{n-2}F^{a\,\xi}_{+}$$

Dipole DIS cross-section can be written as

$$\sigma^{\gamma^* p}(x_B, Q^2) = \int d\nu\, F(\nu)\, x_B^{-\aleph(\nu)-1}\left(\frac{Q^2}{P^2}\right)^{\frac{1}{2}+i\nu}$$

$-q^2 = Q^2 \gg P^2$, and $s = (P+q)^2 \gg Q^2$

$\aleph(\gamma)$ BFKL pomeron intercept. $\gamma = \frac{1}{2} + i\nu$

The n-th moment of the structure function is

$$\int_0^1 dx_B\, x_B^{n-1}\sigma^{\gamma^* p}(x_B, Q^2) = \int_{\frac{1}{2}-i\infty}^{\frac{1}{2}+i\infty} d\gamma\, \frac{F(\gamma)}{n-1-\aleph(\gamma)}\left(\frac{Q^2}{P^2}\right)^{\gamma}$$

Integrating over γ-parameter we get the anomalous dimensions of the leading and higher twist operators at the *unphysical point* $n = 1$.

Analytic continuation

$$\int_0^1 dx_B\, x_B^{n-1} \sigma^{\gamma^* p}(x_B, Q^2) = \int_{\frac{1}{2}-i\infty}^{\frac{1}{2}+i\infty} d\gamma\, \frac{F(\gamma)}{\omega - \aleph(\gamma)} \left(\frac{Q^2}{P^2}\right)^\gamma$$

Analytic continuation: $n-1 \to \omega$ complex continuous variable

$\alpha_s \ln \frac{1}{x_B} \sim 1 \quad \to \frac{\alpha_s}{\omega} \sim 1 \qquad x_B \to 0 \quad \Leftrightarrow \quad \omega \to 0$

$\Rightarrow$ Residues $\omega = \aleph(\gamma)$; expand $\aleph(\gamma)$ for small γ and solve for γ

$$\gamma(\alpha_s, \omega) = \frac{\alpha_s N_c}{\pi\omega} + \mathcal{O}(\alpha_s^2), \quad F(\omega, Q^2) \sim \left(\frac{Q^2}{P^2}\right)^{\frac{\alpha_s N_c}{\pi\omega}}$$

Thus, we get the analytic continuation of anomalous dimension at the *unphysical point* $j \to 1$ of twist-2 gluon operator $F^a_{\xi+} \nabla^{-1} F^{\xi a}{}_{+}$

Light-ray operator

Analytic continuation of light-ray operators at $j = 1$ (or $\omega \to 0$)

$$F^a_{\xi+}(x)\nabla_+^{j-2}F^{a\,\xi}_{+}(x)\Big|_{x=0} = \frac{\Gamma(2-j)}{2\pi i}\int_0^{+\infty} du\; u^{1-j}\, F^a_{\xi+}(0)[0,un]^{ab}F^{b\,\xi}_{+}(un)$$

OPE in light-ray operators in QCD (Balitsky, Braun (1989))

2-point function in BFKL limit (Balitsky; Balitsky, Kazakov, Sobkov (2013-2018))

2-point function in triple Regge limit (Balitsky 2018)

Light-ray operators in CFT (e.g. Kravchuk, Simmons-Duffin (2018))

multiplicatively renorm. light-ray operators in $\mathcal{N}$=4 SYM

$$S_1^j = \mathcal{O}_g^j + \frac{1}{4}\mathcal{O}_\lambda^j - \frac{1}{2}\mathcal{O}_\phi^j \,,$$

$$S_2^j = \mathcal{O}_g^j - \frac{1}{4(j-1)}\mathcal{O}_\lambda^j + \frac{j+1}{6(j-1)}\mathcal{O}_\phi^j \,,$$

$$S_3^j = \mathcal{O}_g^j - \frac{j+2}{2(j-1)}\mathcal{O}_\lambda^j - \frac{(j+1)(j+2)}{2j(j-1)}\mathcal{O}_\phi^j \,,$$

with anomalous dimensions (Lipatov et al. 2004)

$$\gamma_j^{S_1} = 4[\psi(j-1) + \gamma_E] + O(\alpha_s^2), \quad \gamma_j^{S_2} = \gamma_{j+2}, \quad \gamma_j^{S_3} = \gamma_{j+4}^{S_1}$$

In the BFKL limit these are UV divergent.

Point splitting regulator

$x^\mu = x^+ \sqrt{s/2}\, p_1^\mu + x^- \sqrt{s/2}\, p_2^\mu + x_\perp^\mu$ with $2p_1 \cdot p_2 = s$

$$\mathcal{F}^j_{p_1}(x_\perp, y_\perp) = \int_0^{+\infty} du^{1-j} \mathcal{F}_{p_1}(u; x_\perp, y_\perp)$$

$$\mathcal{F}_{p_1}(u; x_\perp, y_\perp) = \int dv F^a{}_{p_1 i}(up_1 + vp_1 + x_\perp) \times [up_1 + vp_1 + x_\perp, vp_1 + y_\perp]^{ab} F^b{}_{p_1}{}^i(vp_1 + y_\perp)$$

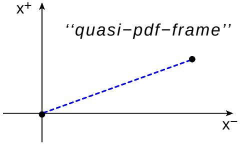

with point splitting

$$\mathcal{S}_1^j = \mathcal{F}^j + \frac{j-1}{4}\Lambda^j - j(j-1)\frac{1}{2}\Phi^j\,,$$
$$\mathcal{S}_2^j = \mathcal{F}^j - \frac{1}{4}\Lambda^j + \frac{j(j+1)}{6}\Phi^j\,,$$
$$\mathcal{S}_3^j = \mathcal{F}^j - \frac{j+2}{2}\Lambda^j - \frac{(j+1)(j+2)}{2}\Phi^j\,.$$

Forward matrix elements

Notice that the coefficients in the S operators are different from the ones in $\mathcal{S}$ operators.

Analytic continuation of the quark twist-two operator

$\gamma = \frac{1}{2} + i\nu$

$$\int_{x_\perp^2 M_N}^{+\infty} dL\, L^{-j}\, \frac{1}{2P^-} \langle P|\bar{\psi}(L, x_\perp)\gamma^-[nL + x_\perp, 0]\psi(0)|P\rangle$$

$$= \int_{\Delta_\perp^2 M_N}^{+\infty} dL\, L^{-j} \frac{N_c}{\pi^3 \Delta_\perp^2} \int_{-\infty}^{+\infty} d\nu \left(\frac{Q_s^2 \Delta_\perp^2}{4}\right)^{\gamma} \frac{\Gamma^3(1+\gamma)\Gamma^2(1-\gamma)}{\Gamma(2+2\gamma)}$$

$$\times \left(-\frac{2}{\Delta_\perp^2} \frac{{P^-}^2 L^2}{M_N^2} + i\epsilon\right)^{\frac{\aleph(\gamma)}{2}}$$

Analytic continuation of the quark twist-two operator

$$\int_{-\infty}^{+\infty} d\nu \;\rightarrow\; \int_{\frac{1}{2}-i\infty}^{\frac{1}{2}+i\infty} d\gamma$$

$$\int_{x_\perp^2 M_N}^{+\infty} dL\, L^{-j} \frac{1}{2P^-} \langle P|\bar{\psi}(L, x_\perp)\gamma^-[nL + x_\perp, 0]\psi(0)|P\rangle$$
$$= \int_{\Delta_\perp^2 M_N}^{+\infty} dL\, L^{-j} \frac{N_c}{\pi^3 \Delta_\perp^2} \int_{\frac{1}{2}-i\infty}^{\frac{1}{2}+i\infty} d\gamma \left(\frac{Q_s^2 \Delta_\perp^2}{4}\right)^{\gamma} \frac{\Gamma^3(1+\gamma)\Gamma^2(1-\gamma)}{\Gamma(2+2\gamma)}$$
$$\times \left(-\frac{2}{\Delta_\perp^2} \frac{P^{-2} L^2}{M_N^2} + i\epsilon\right)^{\frac{\aleph(\gamma)}{2}}$$

Performing the Mellin transform

$$\int_{\Delta_\perp^2 M_N}^{+\infty} dL\, L^{-j} \int_0^{+\infty} dx^+ \int_{-\infty}^{0} dy^+ \delta(x^+ - y^+ - L)$$
$$\times \langle \bar{\psi}(x^+, x_\perp)\gamma^-[x^+ n^\mu + x_\perp, y^+ n^\mu + y_\perp]\psi(y^+, y_\perp)\rangle$$
$$= \frac{N_c}{\pi^3 \Delta_\perp^2} \int_{\frac{1}{2}-i\infty}^{\frac{1}{2}+i\infty} d\gamma\, \theta(\Re[\omega - \aleph(\gamma)]) \frac{(\Delta_\perp^2 M_N)^{-\omega+\aleph(\gamma)}}{\omega - \aleph(\gamma)} \left(\frac{Q_s^2 \Delta_\perp^2}{4}\right)^{\gamma}$$
$$\times \frac{\Gamma^3(1+\gamma)\Gamma^2(1-\gamma)}{\Gamma(2+2\gamma)} \left(-\frac{2}{\Delta_\perp^2}\frac{P^{-2}}{M_N^2} + i\epsilon\right)^{\frac{\aleph(\gamma)}{2}}$$

Taking residue for $\omega - \aleph(\tilde{\gamma}) = 0$ and then perform the Inverse Mellin transform we get back the BFKL resummed result

Instead, assume overlapping regime DGLAP-BFKL

$\Rightarrow \quad \frac{\alpha_s}{\omega} \sim 1 \quad \to \quad \alpha_s \ll \omega \ll 1$

Pseudo quark PDF: leading twists vs BFKL resummation

Leading and next-to-leading twist

$$Q_{\rm p}(x_B,z^2) \simeq \frac{Q_s^2\sigma_0}{24\pi^2\alpha_s x_B}\left(\frac{\bar\alpha_s\left|\ln\frac{Q_s|x_\perp|}{2}\right|}{\ln\left(\frac{2}{x_\perp^2 x_B^2 M_N^2}\right)}\right)^{\frac{1}{2}}\left(1+\frac{Q_s^2x_\perp^2}{5}\right)I_1(v)$$

$$v \equiv \left[4\bar\alpha_s\left|\ln\frac{Q_s|x_\perp|}{2}\right|\ln\left(\frac{2}{x_\perp^2 x_B^2 M_N^2}\right)\right]^{\frac{1}{2}}$$

BFKL resummation

$$Q_{\rm p}(x_B,z^2) \simeq -\frac{iN_cQ_s\sigma_0\bar\alpha_s\ln 2}{32|z||x_B|}\frac{e^{\frac{-\ln^2\frac{Q_s|z|}{2}}{7\zeta(3)\bar\alpha_s\ln\left(\frac{2}{x_B^2z^2M_N^2}+i\epsilon\right)}}}{\sqrt{7\zeta(3)\bar\alpha_s\ln\left(\frac{2}{x_B^2z^2M_N^2}+i\epsilon\right)}}\left(\frac{2}{x_B^2z^2M_N^2}+i\epsilon\right)^{\bar\alpha_s 2\ln 2}$$

Pseudo quark PDF: leading twists vs BFKL resummation

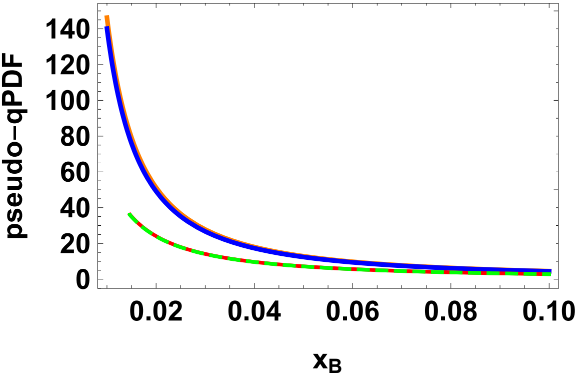

Figure : The plot presents the quark pseudo PDF by comparing the numerical evaluation (illustrated by the orange curve) with its saddle point approximation (portrayed by the blue curve). Furthermore, we display the leading twist (LT) (marked by the green dashed curve) and the next-to-leading twist (NLT) (signified by the solid red curve).

quasi gluon PDF

Leading + next-to-leading twist

$$G_{\mathrm{q}}(x_B, P_\xi) \simeq -\frac{N_c^2\, Q_s^2\, \sigma_0}{16\bar{\alpha}_s^2\pi^3}\frac{1}{2\pi i}\int_{1-i\infty}^{1+i\infty} d\omega \left(-\frac{2P_\xi^2}{M_N^2}+i\epsilon\right)^{\frac{\omega}{2}}\left(-\frac{4P_\xi^2 x_B^2}{Q_s^2}+i\epsilon\right)^{\frac{\bar{\alpha}_s}{\omega}}\left(\omega+\frac{2\bar{\alpha}_s Q_s^2}{5}\frac{1}{P_\xi^2 x_B^2}\right)$$

BFKL resummation

$$Q_{\mathrm{q}}(x_B, P_\xi) \simeq \frac{i N_c P_\xi Q_s \sigma_0}{64\pi}\left(-\frac{2P_\xi^2}{M_N^2}+i\epsilon\right)^{\bar{\alpha}_s 2\ln 2}\int_{-\infty}^{+\infty}\frac{d\varsigma}{|\varsigma|}\, e^{-i\varsigma P_\xi x_B}\frac{e^{-\frac{\ln^2\frac{Q_s|\varsigma|}{2}}{7\zeta(3)\bar{\alpha}_s\ln\left(-\frac{2P_\xi^2}{M_N^2}+i\epsilon\right)}}}{\sqrt{7\zeta(3)\bar{\alpha}_s\ln\left(-\frac{2P_\xi^2}{M_N^2}+i\epsilon\right)}}$$

Usual exponentiation of the BFKL pomeron intercept, which resums logarithms of x_B, is missing.

For low values of x_B and fixed values of P these corrections are enhanced rather than suppressed at this regime.

Here $P_\xi = 4$ GeV.

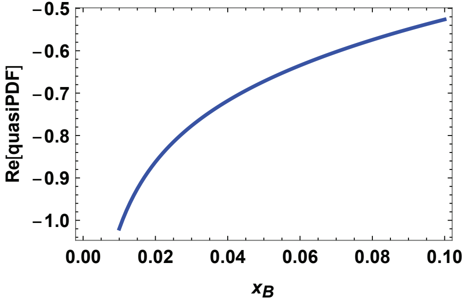

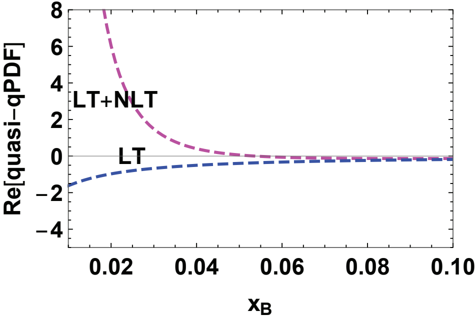

Left plot show BFKL resumed quark quasi-PDF; right plot is LT and NLT

Quasi-PDF have rather unusual behavior at low-x_B.

Ioffe-time distribution with photon impact factor

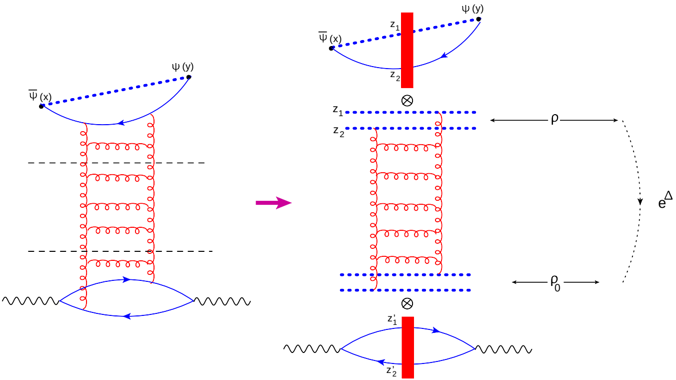

Figure : Here we diagrammatically illustrate the high-energy OPE with the photon impact factor model. The two black dashed lines represent the factorization in rapidity. The diagram at the bottom of the right panel is the diagram for the photon impact factor.

Ioffe-time distribution with photon impact factor

$$\left\langle \frac{z^\alpha}{|z|}\bar\psi(x)\gamma_\alpha[x,y]\psi(y)\right\rangle \varepsilon^{\lambda,\,\mu}\varepsilon^{\lambda,\,\nu *}\int d^4x' d^4y'\, e^{iq\cdot(x'-y')} j^\mu(x') j^\nu(y') \Big\rangle$$

$$= \frac{i\bar\alpha_s^2}{32|Q||\Delta_\perp|}\frac{9\pi^3\sqrt{\pi}}{512}\frac{e^{\frac{-\ln^2\frac{Q^2\Delta_\perp^2}{4}}{7\zeta(3)\bar\alpha_s\ln\left(-\frac{2\sqrt{2}\varrho^2}{\Delta_\perp^2 Q^2}+i\epsilon\right)}}}{\sqrt{7\zeta(3)\bar\alpha_s\ln\left(-\frac{2\sqrt{2}\varrho^2}{\Delta_\perp^2 Q^2}+i\epsilon\right)}}\left(-\frac{2\sqrt{2}\varrho^2}{\Delta_\perp^2 Q^2}+i\epsilon\right)^{\bar\alpha_s 2\ln 2}$$

Ioffe-time amplitude at LT and NLT with photon impact factor

$$\frac{1}{2\pi i}\int_{1-i\infty}^{1+i\infty} d\omega\, L^{\omega}\int_{\Delta_\perp^2\,\Delta E}^{+\infty} dL\, L^{-j}$$
$$\times\frac{z^\alpha}{|z|}\left\langle\bar{\psi}(x)\gamma_\alpha[x,y]\psi(y)\varepsilon^{\lambda,\,\mu}\varepsilon^{\lambda,\,\nu*}\int d^4x' d^4y'\, e^{iq\cdot(x'-y')}j_\mu(x')j_\nu(y')\right\rangle$$
$$=\frac{i}{288\pi}\frac{2\bar{\alpha}_s\ln\frac{4}{Q^2\Delta_\perp^2}}{\ln\left(-\frac{2\sqrt{2}\varrho^2}{\Delta_\perp^2 Q^2}+i\epsilon\right)}I_2(h)\left(1-\frac{3}{50}\frac{Q^2\Delta_\perp^2}{4}\right)$$

$$h=\left[2\bar{\alpha}_s\ln\frac{4}{Q^2\Delta_\perp^2}\ln\left(-\frac{2\sqrt{2}\varrho^2}{\Delta_\perp^2 Q^2}+i\epsilon\right)\right]^{\frac{1}{2}}$$

Plot of the Ioffe-time amplitude at LT and NLT with photon impact factor

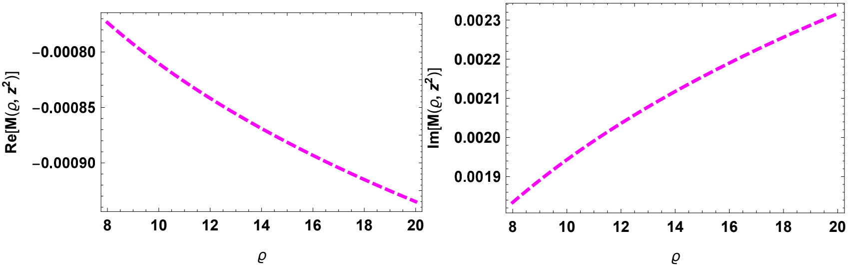

Figure : In the left and right panel we plot the real and imaginary part, respectively of the Ioffe-time amplitude at the leading twist.

Lattice calculation: results

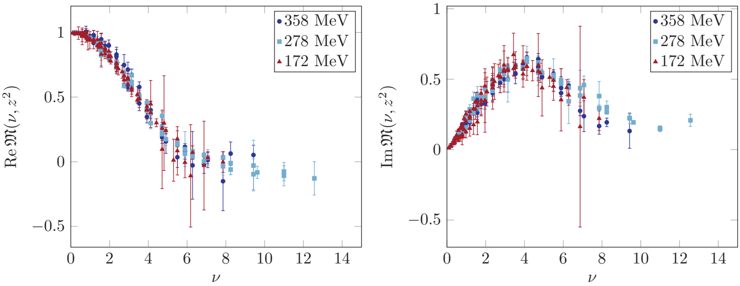

Phys.Rev.Lett. 125 (2020) 23, 232003

Ioffe-time $\nu \equiv z \cdot P$ z^μ space-like vector $i = 1, 2$

This talk: $\nu \to \varrho$

Large Ioffe-time behavior is governed by higher-twists contributions which are not capture by Lattice calculation

Conclusions

- Large-distance behavior of the gluon Ioffe-time distribution is computed
  - Ioffe-time ϱ acts as rapidity parameter.
    - $\alpha_s \ln \varrho$ resumed by BFKL eq.

- Pseudo-PDF and quasi-PDF have a very different behavior at low-x_B.
  - pseudo-PDF have typical rising behavior at low-x_B.
  - quasi-PDF have rather unusual behavior at low-x_B.
    - usual exponentiation of the BFKL pomeron intercept, which resums logarithms of x_B, is missing.

- The power corrections in the quasi-PDF do not come in as inverse powers of P but as inverse powers of $x_B P$
  - for low values of x_B and fixed values of P these corrections are enhanced rather than suppressed at this regime.